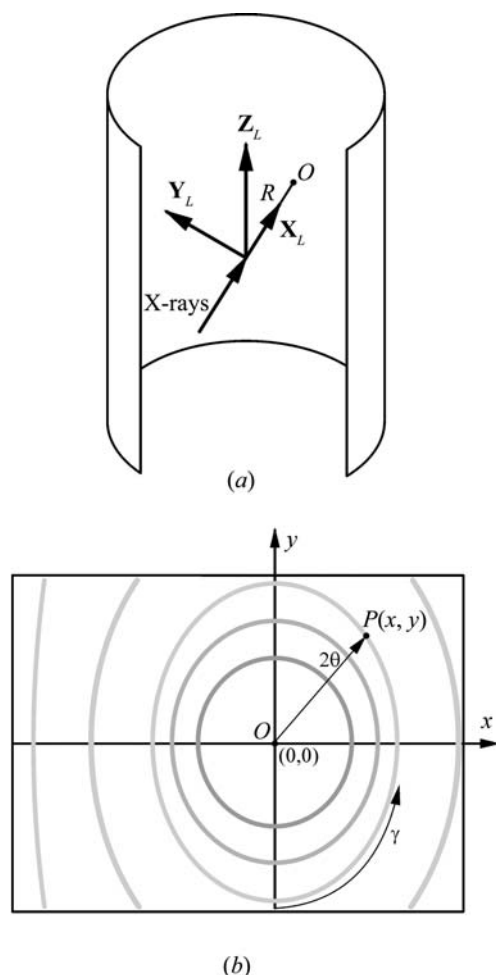


## 2. INSTRUMENTATION AND SAMPLE PREPARATION


**Figure 2.5.6**

Cylinder-shaped detector in vertical direction: (a) detector position in the laboratory coordinates; (b) pixel position in the flattened image.

$$2\theta = \arccos \frac{x \sin \alpha + D \cos \alpha}{(D^2 + x^2 + y^2)^{1/2}} \quad (0 < 2\theta < \pi), \quad (2.5.6)$$

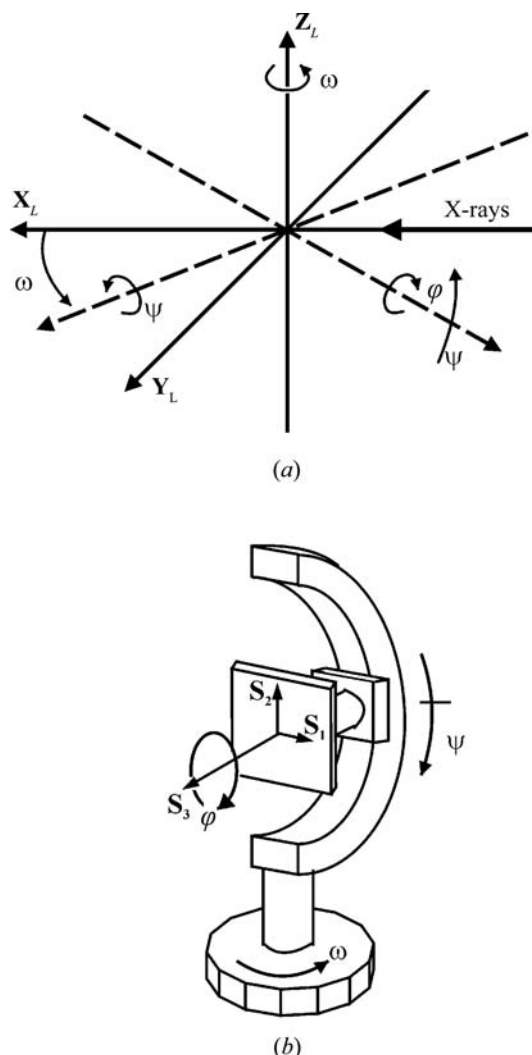
$$\gamma = \frac{x \cos \alpha - D \sin \alpha}{|x \cos \alpha - D \sin \alpha|} \arccos \frac{-y}{[y^2 + (x \cos \alpha - D \sin \alpha)^2]^{1/2}} \quad (-\pi < \gamma \leq \pi). \quad (2.5.7)$$

### 2.5.2.2.3. Pixel position in diffraction space for a curved detector

The conic sections of the diffraction cones with a curved detector depend on the shape of the detector. The most common curved detectors are cylinder-shaped detectors. The diffraction frame measured by a cylindrical detector can be displayed as a flat frame, typically a rectangle. Fig. 2.5.6(a) shows a cylindrical detector in the vertical direction and the corresponding laboratory coordinates  $X_L, Y_L, Z_L$ . The sample is located at the origin of the laboratory coordinates inside the cylinder. The incident X-rays strike the detector at a point  $O$  if there is no sample or beam stop to block the direct beam. The radius of the cylinder is  $R$ . Fig. 2.5.6(b) illustrates the 2D diffraction image collected with the cylindrical detector. We take the point  $O$  as the origin of the pixel position  $(0, 0)$ . The diffraction-space coordinates  $(2\theta, \gamma)$  for a pixel at  $P(x, y)$  are given by

$$2\theta = \arccos \left[ R \cos \left( \frac{x}{R} \right) / (R^2 + y^2)^{1/2} \right], \quad (2.5.8)$$

$$\gamma = \frac{x}{|x|} \arccos \left\{ -y / \left[ y^2 + R^2 \sin^2 \left( \frac{x}{R} \right) \right]^{1/2} \right\} \quad (-\pi < \gamma \leq \pi). \quad (2.5.9)$$


**Figure 2.5.7**

Sample rotation and translation. (a) Three rotation axes in laboratory coordinates; (b) rotation axes  $(\omega, \psi, \varphi)$  and sample coordinates.

The pixel-position-to- $(2\theta, \gamma)$  conversion for detectors of other shapes can also be derived. Once the diffraction-space coordinates  $(2\theta, \gamma)$  of each pixel in the curved 2D detector are determined, most data-analysis algorithms developed for flat detectors are applicable to a curved detector as well.

### 2.5.2.2.3. Sample space and goniometer geometry

#### 2.5.2.2.3.1. Sample rotations and translations in Eulerian geometry

In a 2D-XRD system, three rotation angles are necessary to define the orientation of a sample in the diffractometer. These three rotation angles can be achieved either by a Eulerian geometry, a kappa ( $\kappa$ ) geometry or another kind of geometry. The three angles in Eulerian geometry are  $\omega$  (omega),  $\psi$  (psi) and  $\varphi$  (phi). Fig. 2.5.7(a) shows the relationship between rotation axes  $(\omega, \psi, \varphi)$  in the laboratory system  $X_L, Y_L, Z_L$ . The  $\omega$  angle is defined as a right-handed rotation about the  $Z_L$  axis. The  $\omega$  axis is fixed in the laboratory coordinates. The  $\psi$  angle is a right-handed rotation about a horizontal axis. The angle between the  $\psi$  axis and the  $X_L$  axis is given by  $\omega$ . The  $\psi$  axis lies on  $X_L$  when  $\omega$  is set at zero. The  $\varphi$  angle defines a left-handed rotation about an axis on the sample, typically the normal of a flat sample. The  $\varphi$  axis lies on the  $Y_L$  axis when  $\omega = \psi = 0$ . In an aligned diffraction system, all three rotation axes and the primary X-ray beam cross at the

## 2.5. TWO-DIMENSIONAL POWDER DIFFRACTION

origin of the  $X_L, Y_L, Z_L$  coordinates. This cross point is also known as the goniometer centre or instrument centre.

Fig. 2.5.7(b) shows the relationship and stacking sequence among all rotation axes ( $\omega, \psi, \varphi$ ) and the sample coordinates  $S_1, S_2, S_3$ .  $\omega$  is the base rotation; all other rotations and translations are on top of this rotation. The next rotation above  $\omega$  is the  $\psi$  rotation. The next rotation above  $\omega$  and  $\psi$  is the  $\varphi$  rotation. The sample coordinates  $S_1, S_2, S_3$  are fixed to the sample regardless of the particular sample orientation given by the rotation angles ( $\omega, \psi, \varphi$ ). The  $\varphi$  rotation in the goniometer is intentionally chosen as a left-handed rotation so that the diffraction vectors will make a right-hand rotation observed in the sample coordinates  $S_1, S_2, S_3$ .

### 2.5.2.4. Diffraction-vector transformation

#### 2.5.2.4.1. Diffraction unit vector in diffraction space and sample space

In 2D-XRD data analysis, it is crucial to know the diffraction-vector distribution in terms of the sample coordinates  $S_1, S_2, S_3$ . However, the diffraction-vector distribution corresponding to the measured 2D data is always given in terms of the laboratory coordinates  $X_L, Y_L, Z_L$  because the diffraction space is fixed to the laboratory coordinates. Fig. 2.5.8 shows the unit vector of a diffraction vector in both (a) the laboratory coordinates  $X_L, Y_L, Z_L$  and (b) the sample coordinates  $S_1, S_2, S_3$ . In Fig. 2.5.8(a) the unit vector  $\mathbf{h}_L$  is projected to the  $X_L, Y_L$  and  $Z_L$  axes as  $h_x, h_y$  and  $h_z$ , respectively. The three components are given by equation (2.5.5). In order to analyse the diffraction results relative to the sample orientation, it is necessary to transform the unit vector to the sample coordinates  $S_1, S_2, S_3$ . Fig. 2.5.8(b) shows the same unit vector, denoted by  $\mathbf{h}_s$  projected to  $S_1, S_2$  and  $S_3$  as  $h_1, h_2$  and  $h_3$ , respectively.

#### 2.5.2.4.2. Transformation from diffraction space to sample space

The transformation of the unit diffraction vector from the laboratory coordinates  $X_L, Y_L, Z_L$  to the sample coordinates  $S_1, S_2, S_3$  is given by

$$\mathbf{h}_s = \mathbf{A}\mathbf{h}_L, \quad (2.5.10)$$

where  $\mathbf{A}$  is the transformation matrix. For Eulerian geometry in matrix form, we have

$$\begin{bmatrix} h_1 \\ h_2 \\ h_3 \end{bmatrix} = \begin{bmatrix} a_{11} & a_{12} & a_{13} \\ a_{21} & a_{22} & a_{23} \\ a_{31} & a_{32} & a_{33} \end{bmatrix} \begin{bmatrix} h_x \\ h_y \\ h_z \end{bmatrix} \\ = \begin{bmatrix} -\sin \omega \sin \psi \sin \varphi & \cos \omega \sin \psi \sin \varphi & -\cos \psi \sin \varphi \\ -\cos \omega \cos \varphi & -\sin \omega \cos \varphi & \\ \sin \omega \sin \psi \cos \varphi & -\cos \omega \sin \psi \cos \varphi & \cos \psi \cos \varphi \\ -\cos \omega \sin \varphi & -\sin \omega \sin \varphi & \\ -\sin \omega \cos \psi & \cos \omega \cos \psi & \sin \psi \end{bmatrix} \\ \times \begin{bmatrix} -\sin \theta \\ -\cos \theta \sin \gamma \\ -\cos \theta \cos \gamma \end{bmatrix}. \quad (2.5.11)$$

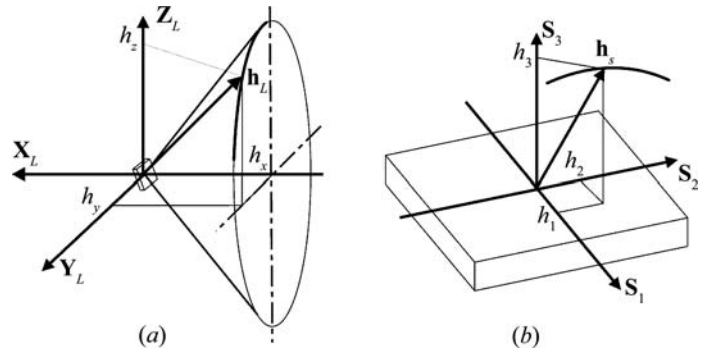


**Figure 2.5.8**

Unit diffraction vector in (a) the laboratory coordinates and (b) the sample coordinates.

In expanded form:

$$\begin{aligned} h_1 &= \sin \theta (\sin \varphi \sin \psi \sin \omega + \cos \varphi \cos \omega) + \cos \theta \cos \gamma \sin \varphi \cos \psi \\ &\quad - \cos \theta \sin \gamma (\sin \varphi \sin \psi \cos \omega - \cos \varphi \sin \omega) \\ h_2 &= -\sin \theta (\cos \varphi \sin \psi \sin \omega - \sin \varphi \cos \omega) \\ &\quad - \cos \theta \cos \gamma \cos \varphi \cos \psi \\ &\quad + \cos \theta \sin \gamma (\cos \varphi \sin \psi \cos \omega + \sin \varphi \sin \omega) \\ h_3 &= \sin \theta \cos \psi \sin \omega - \cos \theta \sin \gamma \cos \psi \cos \omega - \cos \theta \cos \gamma \sin \psi \end{aligned} \quad (2.5.12)$$

In addition to the diffraction intensity and Bragg angle corresponding to each data point on the diffraction ring, the unit vector  $\mathbf{h}_s\{h_1, h_2, h_3\}$  provides orientation information in the sample space. The transformation matrix of any other goniometer geometry, such as kappa geometry (Paciorek *et al.*, 1999), can be introduced into equation (2.5.10) so that the unit vector  $\mathbf{h}_s\{h_1, h_2, h_3\}$  can be expressed in terms of the specified geometry. All equations using the unit vector  $\mathbf{h}_s\{h_1, h_2, h_3\}$  in this chapter, such as in data treatment, texture analysis and stress measurement, are applicable to all goniometer geometries provided that the unit-vector components are generated from the corresponding transformation matrix from diffraction space to the sample space.

#### 2.5.2.4.3. Transformation from detector space to reciprocal space

Reciprocal-space mapping is commonly used to analyse the diffraction patterns from highly oriented structures, diffuse scattering from crystal defects, and thin films (Hanna & Windle, 1995; Mudie *et al.*, 2004; Smilgies & Blasini, 2007; Schmidbauer *et al.*, 2008). The equations of the unit-vector calculation given above can also be used to transform the diffraction intensity from the diffraction space to the reciprocal space with respect to the sample coordinates. The direction of the scattering vector is given by the unit vector  $\mathbf{h}_s\{h_1, h_2, h_3\}$  and the magnitude of the scattering vector is given by  $2 \sin \theta / \lambda$ , so that the scattering vector corresponding to a pixel is given by

$$\mathbf{H} = \frac{2 \sin \theta}{\lambda} \mathbf{h}_s. \quad (2.5.13)$$

The three-dimensional reciprocal-space mapping can be obtained by applying the normalized pixel intensities to the corresponding reciprocal points. With various sample orientations, all pixels on the detector can be mapped into a 3D reciprocal space.